EXPERIMENTAL STUDY OF MASONRY INFILLED RC FRAMES CONSIDERING THE INFLEUNCE OF VARYING FRAME AND MASONRY STRENGTH

Hamood ALWASHALI[1)], Yuta TORIHATA[2)], Kiwoong JIN [3)] and Masaki MAEDA [4)]

1) JAEE student member, Ph.D. candidate, Graduate School of Engineering, Dept. of Architectural and Building Science, Sendai, Japan, Hamood@rcl.archi.tohoku.ac.jp
2) JAEE student member, graduate student, Graduate School of Engineering, Dept. of Architectural and Building Science, Sendai, Japan, Torihata@rcl.archi.tohoku.ac.jp
3) JAEE member, Ph.D., Assistant Professor, Graduate School of Engineering, Dept. of Architectural and Building Science, Sendai, Japan, Jin@rcl.archi.tohoku.ac.jp
4) JAEE member, Ph.D., Professor, Graduate School of Engineering, Dept. of Architectural and Building Science, Sendai, Japan, Maeda@rcl.archi.tohoku.ac.jp

ABSTRACT: This study focuses on the in-plane behavior of unreinforced masonry (URM) infill walls installed in reinforced concrete (RC) frames. Three specimen ½ scale specimens with different RC frames and masonry infill walls were tested using a static cyclic loading protocol. The main objective was investigating the influence of changing masonry strength to seismic capacity in terms of: strength, stiffness and deformation limits. Results of the presented experiment show that as the ratio of frame shear strength to masonry shear strength increases, there was great improvement of the masonry infill walls in terms of strength and avoidance of sudden brittle behaviour of the masonry infill. However, varying frame strength did not significantly influence the initial stiffness and story drift at max strength. The deformation limits of masonry infill were found to be directly proportional to both the compressive prism strength of the masonry infill and the ratio of shear strength of frame to that of the masonry infill. In addition, the specimen with masonry infill using low mortar strength showed greater ductile behaviour and relatively less damage observed in masonry infill panel.

Key Words: Masonry infill wall, RC frame, Seismic performance evaluation, Static cyclic loading test. Ratio of shear strength of frame to masonry infill

1. INTRODUCTION.

Many of the reinforced concrete buildings in the world and particularly in developing countries use masonry infill as partition walls. The influence of masonry on the structural behavior was recognized from the experience of earthquake disasters and experiments by several researchers (i.e., Priestly et al. [1)]). In general, masonry infill increases the frame strength, which is considered as a beneficial point. On the other hand, masonry infill exerts reaction forces on the RC frame causing additional moment and shear forces, which results in unexpected failure modes (FEMA 306 [2)]). In addition, the masonry infill greatly increases the frame stiffness that might change the seismic demand due to significant

reduction in natural period of the building. Despite of these distinctive characteristics, many practicing engineers still assume that the walls are non-structural elements due to incomplete knowledge concerning RC frames with masonry infill behavior and complexity in evaluating their failure modes. The seismic performance of masonry infill depends on several parameters such as the confinement effect, masonry type, aspect ratio, mortar strength. Among these factors, the relative strength of the boundary RC frame to the masonry infill is a crucial parameter that not only governs the behavior and failure modes of the RC frame but also the strength and failure mode of the masonry infill. This was demonstrated in an experimental study conducted by Mehrabi et al[3]. A study by Wood[4] emphasized the impact of frame to masonry infill strength ratio on failure mechanism and proposed empirical equations to calculate shear strength based on this ratio. However, in another proposed empirical equation by Mainstone[5], which was also adopted by FEMA 306[2], greater emphasis was placed on the frame to infill stiffness ratio rather than strength in controlling the equivalent strut width which is used to calculate frame strength and initial stiffness. On the other hand, Liauw et al[6] proposed different diagonal compression failure modes of the infill based on plastic collapse theory. The proposed equations are directly related to the ratio of frame to masonry infill strength and the stiffness ratio is not taken into account. Sanjenied[7] proposed analysis methods based on the contact length between the frame and masonry infill which is controlled by the ratio of frame strength to masonry infill strength. However, based on extensive experimental data, Flangan et al[8] concluded that the strength of compression failure mechanism of the masonry infill is not significantly influenced by the frame to masonry infill strength or stiffness ratios and instead proposed simplified empirical equations which did not use either ratio. ASCE/SEI 41[9] proposed equations to calculate the masonry infill strength based on shear tests of masonry infill ignoring the frame to masonry infill strength ratio.

In summary, the experimental results and equations proposed by various researchers tend to contradict each other. Some studies place emphasis on the importance of the frame to infill strength ratio while others emphasize the importance of the frame to infill stiffness ratio and others ignore the influence of these ratios altogether. Therefore, this study aims to clarifying seismic capacity of masonry infill when changing surrounding frame strength and varying masonry mortar strength. The influence of frame to infill strength and stiffness ratios on the strength, stiffness and deformation limits is investigated by testing three ½ scale specimens with different RC frames and masonry infill using a static cyclic loading protocol.

2. EXPERIMENTAL PROGRAM

2.1 Test specimens

Three half-scaled specimens with different RC frames, having unreinforced masonry infills are designed. The main variance parameter for test specimens is the ratio of the boundary frame to masonry infill lateral strength defined as β index, as shown in Eq. (1). Specimens are named WF (weak frame), WM (weak mortar) and SF (strong frame) with β of 0.4, 0.8 and 1.5, respectively.

$$\beta = V_f / V_{\text{inf}} \tag{1}$$

Where V_f is the boundary frame lateral strength which is calculated to be the ultimate flexural capacity of a bare frame with plastic hinges at top and bottom of columns. The V_{inf} is the masonry infill lateral strength calculated based on Eq. (2) which is a simplified empirical equation showing good agreement with experimental database studied by the author (Al-Washali et al. [10])

$$V_{\text{inf}} = 0.05\, fm \cdot t_{\text{inf}} \cdot l_{\text{inf}} \tag{2}$$

Where fm is the compressive strength of masonry prism, t_{inf} is the infill thickness, l_{inf} is infill length.
The specimen dimensions and details are shown in Fig. 1. Both specimens are identical except for the column size and reinforcement, as shown in Fig 1. The beams were designed to be stronger and stiff enough to simulate a typical case of a weak column and strong beam system observed in existing buildings of old designs.

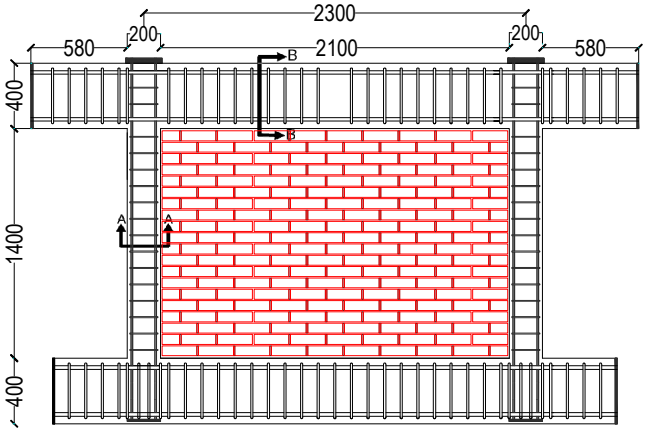

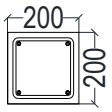

Column
200x200mm
(Specimen WF)
Main bars; 4-D10
Stirrup; D6 @100

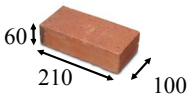

Masonry unit
brick dimensions
for all specimens

a) Specimen WF (Weak frame)

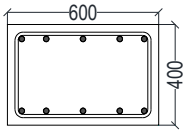

Beam of all specimens 600x400mm
Main bars; 10-D22
Stirrup; D13 @100

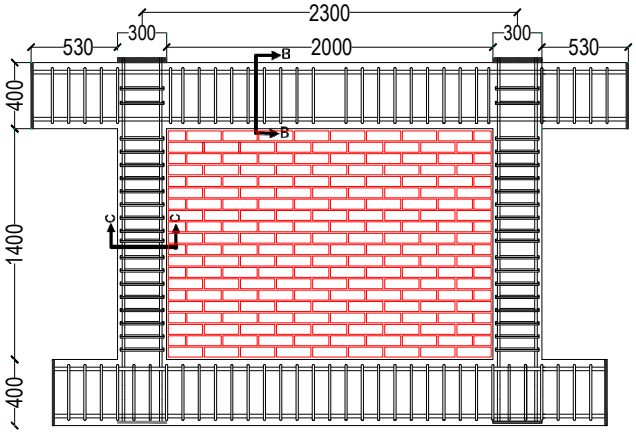

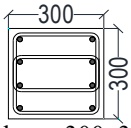

Column 300x300 mm
(Specimen SF)
Main bars;8-D16
Stirrup; D10 @80

b) Specimen SF (Strong frame)

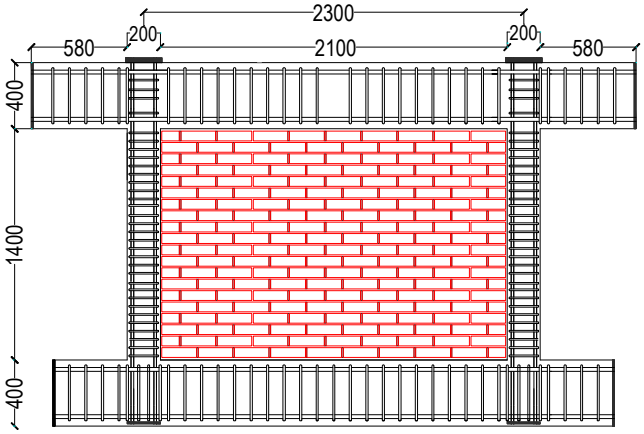

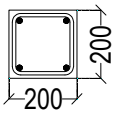

Column 200x200mm
(Specimen WM)
Main bars; 4-D16
Stirrup;D10 @50

b) Specimen WM (Weak Mortar)

Fig. 1. Dimensions and reinforcement of specimens; units in mm

2.2 Material properties

The infill panels are constructed using 60 x 100 x 210 mm solid bricks conventionally used in Japan. A professional mason built the infill, after the frame construction, where its thickness is 100mm and mortar head and bed joint thickness is about 10mm. Table 1 and Table 2 show the properties based on material tests conducted on the reinforcing steel, concrete and masonry respectively, where those values represent the mean values of three samples in each test. These include steel tensile strength by

JIS Z 2201[11], the compression strength of concrete and mortar cylinders by JIS A 1108[11], the splitting tensile strength of concrete and mortar cylinders by JIS A 1113[11], the masonry prism compressive strength tested according to ASTM C1314[12]. The concrete used for both specimens is identical and from the same batch. The proportion of cement and sand for the mortar is 1:2.5 for specimen SF and WF (mass proportion), 1:6 for specimen WM designed with weak mortar. The masonry prism samples were made simultaneously with the infill panel by the same professional mason. The material tests were conducted at the same time with the experimental loading for each specimen individually.

Table 1 Material properties of Concrete and Masonry

Specimen name	Frame Concrete			Masonry Prism			Mortar cylinders	Brick unit
	Compre--sive strength (MPa)	Elastic moduli (MPa)	Split Tensile strength (MPa)	Compres--sive strength (MPa)	Elastic moduli (MPa)	Strain at peak stress	Compres--sive strength (MPa)	Compressive strength (MPa)
WF	24.2	2.3×10^4	2.1	17.3	7840	0.0037	20.2	38.1
SF	28.3	2.3×10^4	2.4	18.6	8140	0.0039	29.2	38.1
WM	25.8	2.3×10^4	2	13.3	4200	0.0084	4.8	38.1

Table 2 Reinforcement mechanical properties

Bar	Nominal strength	Yield strength (MPa)	Ultimate tensile strength (MPa)
D6	SD345	476	595
D10	SD345	384	547
D13	SD345	356	555
D16	SD345	370	556
D22	SD390	447	619

2.3.Test setup and instrumentation

The loading system is shown schematically in Figure 2. The vertical load was applied on RC columns by two vertical hydraulic jacks and was maintained to be 200kN on each column. Two pantograph, attached with the vertical jacks, restricted any torsional and out-of-plane displacement. Two horizontal jacks, applying together an incremental cyclic loading, were attached at the beam level and were controlled by a drift angle of R%, defined as the ratio of lateral story deformation to the story height measured at the middle depth of the beam (h=1,600mm). The lateral loading program consisted of 2 cycles for each peak drift angle of 0.05%, 0.1%, 0.2%, 0.4%, 0.6%, 0.8%, 1%, 1.5% and 2 %.

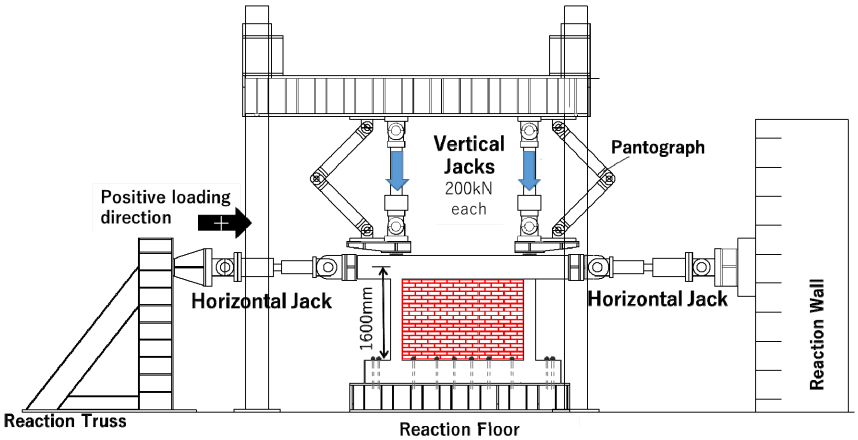

Fig. 2. Test setup (units: mm)

2.4. Experimental results

The lateral load versus story drift angle graphs of both specimens are shown in Figures 3, 4 and 5. Cracks and failure patterns after final drift cycle of 2.0% are shown in Figure 6.

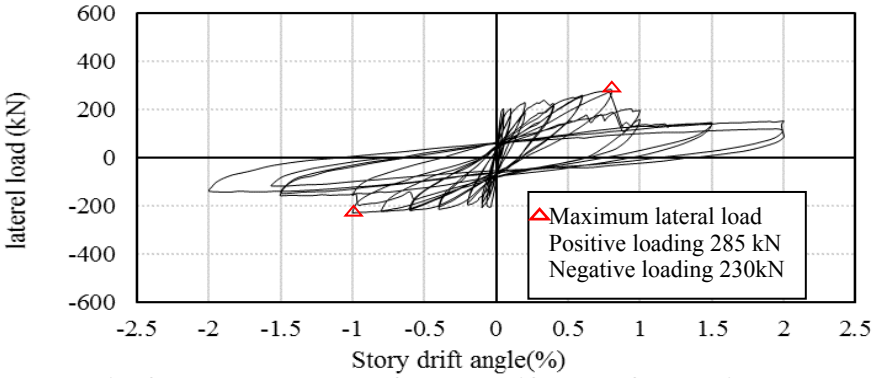

Fig. 3. Lateral strength & story drift angle for specimen WF

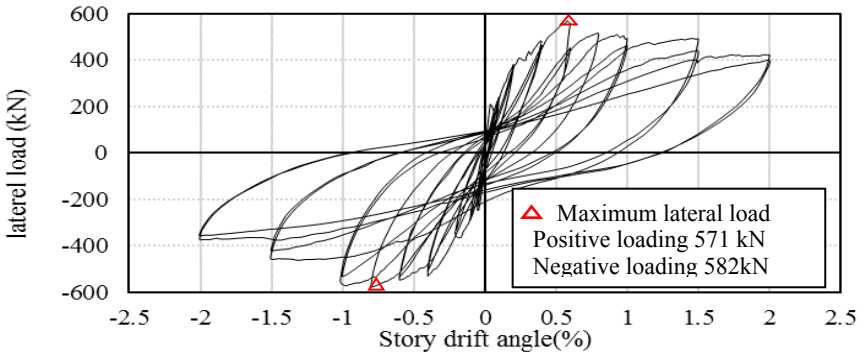

Fig. 4. Lateral strength & story drift angle for specimen SF

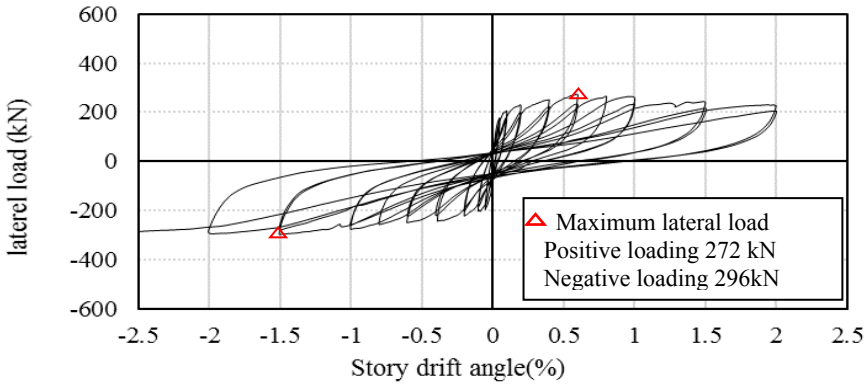

Fig. 5. Lateral strength & story drift angle for specimen WM

For Specimen WF:

Very small cracks on mortar bed joint and diagonal cracks on bricks near loading corner of infill panel, less than 0.3mm width, started at early stages of loading just when the drift angle was 0.05%. At drift angles of 0.2% and 0.4%, the longitudinal reinforcement in the tensile column (windward column) yielded at the upper critical section and above its mid-height, respectively, forming failure mechanism similar to a short column, as illustrated in Figure 7-a). Just after reaching the maximum lateral strength, there was a sudden drop of lateral load bearing capacity with extensive cracking and spalling of bricks. After the drift of 1%, the main failure mechanism changed from diagonal cracks to sliding cracks with clear sliding movement at the mid-height of the infill. At drift story of 2% in the negative cycle, the concrete around the reinforcement of top compression column spalled-off and main bars buckled.

For Specimen SF:
Cracking of infill panel also started at the peak of the first loading cycle, which was relatively similar to the crack width observed in specimen WF at this stage. At drift angle between 0.6% ~ 0.7%, both columns yielded at the locations shown in Figure 7-b). As it reached its maximum strength, the lateral load gradually degraded (contrarily to the sudden degradation of strength in previous specimen WF) with the drift angle increase until the drift angle of 1.5%, where there was a slight drop of the lateral load, after the horizontal sliding between bricks clearly increased. At the drift angle of 2%, the loading stopped as planned, and the masonry infill damage at this point was much greater than observed in the previous specimen WF (see Figure 6-b). In spite that columns had many cracks, there was no extensive damage or spalling of concrete cover.
For Specimen WM:
Contrary to previous specimen with stronger mortar, cracks didn't occur at story drift of 0.05% in specimen WM (weak mortar). Very small cracks at mortar bed joint and diagonal on bricks started to be noticed from 0.1%. At drift angle between 0.6% ~ 0.8%, both columns yielded at the locations shown in Figure 7-b). The lateral load slightly degraded in the positive loading after 1% (contrarily to the sudden degradation of strength in previous specimen WF). However, there was no significant degradation of strength in the negative loading even when specimen reached story drift of 2%. At the drift angle of 2%, the loading stopped as planned, and the masonry infill damage at this point was much less than observed in the previous specimens WF and SF (see Figure 6). In spite that columns had many cracks, there was no extensive damage or spalling of concrete cover.

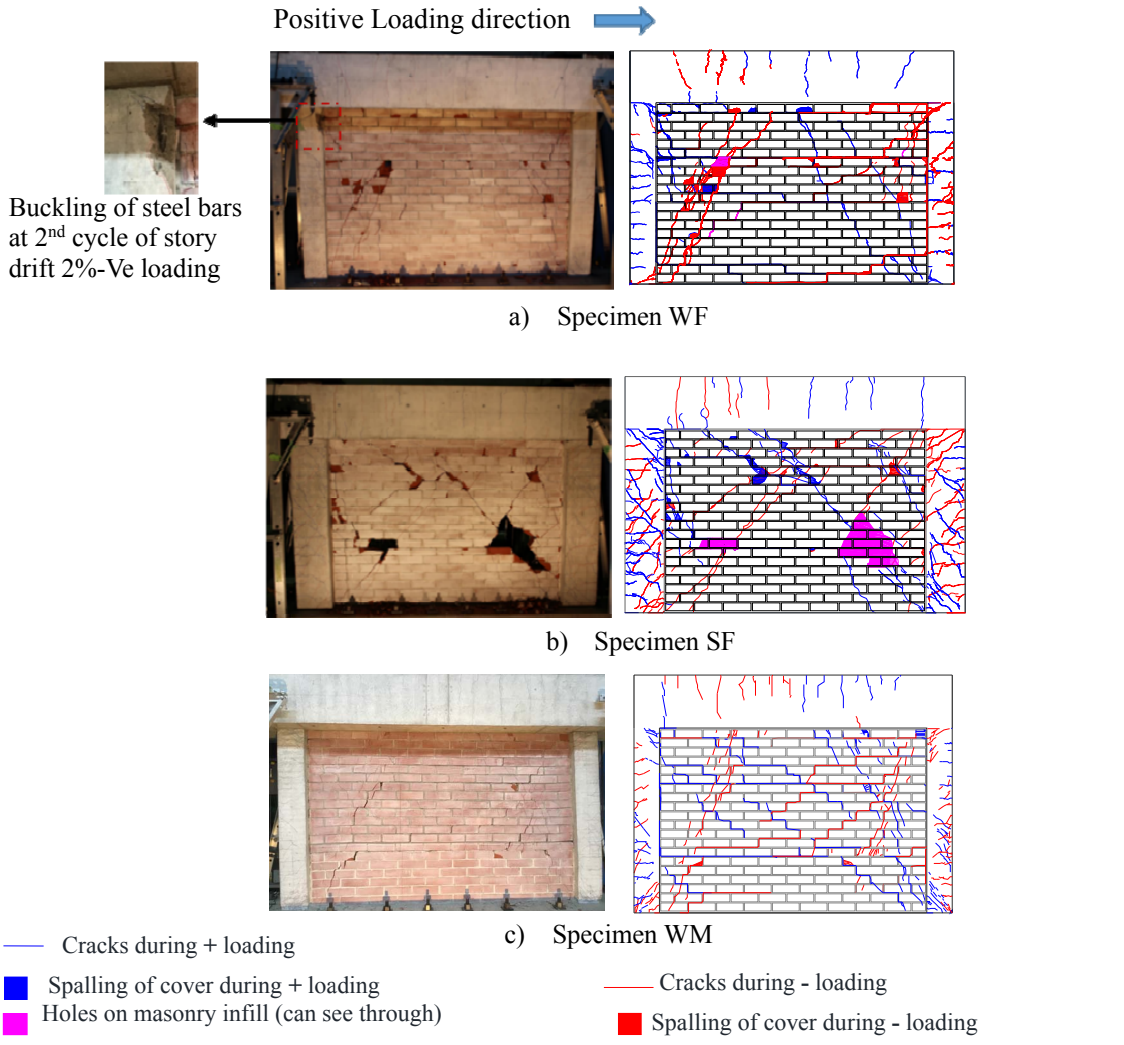

Fig. 6. Crack patterns observed at end of the test for specimens : a) WF b) SF c) WM

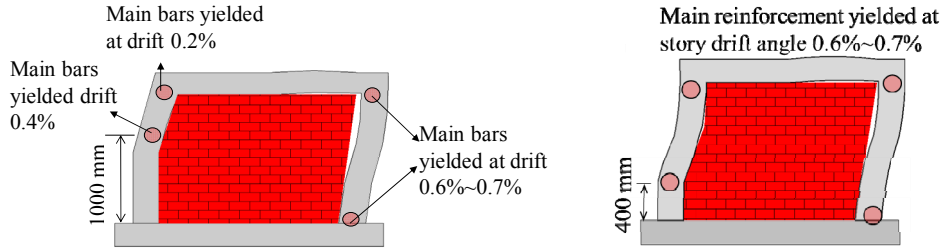

Fig. 7. Hinge locations formed in RC frame: a) specimen WF, b) Specimen SF & WM

3. DISCUSSIONS OF EXPERIMENTAL RESULTS:

3.1 Lateral strength

The maximum lateral load contributed by the masonry infill (V_{inf}) is calculated by deducting the bare frame lateral strength (V_f) from the maximum lateral load of the overall structure (V_{max}), as shown in Eq. (4):

$$V_f = 4M_u/h_o \quad (3)$$

$$V\,\text{inf} = V\,\text{max} - Vf \quad (4)$$

Where M_u is the minimum plastic moment of the column or beam calculated by AIJ provision (2016) and h_o is the clear height of column (taken here as infill height).

Table 3 shows the experimental shear strength of masonry infills in both specimens, which is the shear force (V_{inf}) divided by the infill cross-sectional area. Even though infill panels of specimen WF and SF are made by exactly same material and have similar prism compression strength, specimen SF has the shear capacity of 1.48N/mm^2 which is about 1.5 times the shear strength in specimen WF (0.93 N/mm^2). On the other hand, shear strength of infill panel was not affected much by using very low mortar strength.
The simplified Eq. (2) based on previous study by the author (AlWashali et al.[10]) showed relatively good estimation for specimen WF and WM, but it underestimated that of Specimen SF. This underestimation is considered due to the ignorance of the confinement effect of the strong boundary frame.

Table 3. Maximum lateral load and shear strength of infill

Specimen name	Experiment V_{max}(kN)		Vf (kN) Eq(3)	Experiment V_{inf}(kN) by Eq(4)		Maximum shear strength τ_{inf} (N/mm^2)		Average V_{inf} of both directions (kN)	Average shear strength τ_{inf} of both directions (N/mm^2)
	+ loading	- loading		+ loading	- loading	+ loading	- loading		
WF	285	230	71	214	159	1.07	0.80	186.5	0.93
SF	571	582	280	291	302	1.46	1.51	296.5	1.48
WM	272	296	113	159	183	0.76	0.87	171.2	0.82

3.2 Stiffness:

The initial stiffness K_o of infilled frame is taken as the slope between the origin point of the load-displacement curve and the point with the major visible crack in the masonry infill and the RC frame, which was determined as the story drift of 0.1%. Table 4 shows the comparison between the initial stiffness of overall frames and that of bare frames. Herein, the initial stiffness of bare frame is calculated based on its elastic gross concrete section. The masonry infill greatly increased the initial stiffness up to about 7.1 times that of bare frame in specimen WF. Therefore, in the seismic design, ignoring the contribution of masonry

infill to stiffness and natural period of building may cause non-conservative design practice since buildings with lower natural period have greater seismic forces.
The most well recognized method for calculating the infill stiffness is using the equivalent diagonal compression strut, which has the same elasticity and thickness with the infill panel. Paulay et al. (1992) recommended using the effective width of strut, where W_{ef} and d_m is the diagonal length of infill panel in Eq. (5)

$$W_{ef} = 0.25 d_m \tag{5}$$

Table 4 shows the comparison between experimental and numerical initial stiffness based on the strut width recommended by FEMA 306[2)] and Pualay et al.[1)]. The Strut width calculated by FEMA 306 (1996) underestimates the initial stiffness by about 1.9, 1.08 and 2.35 for specimen WF, specimen SF and specimen WM, respectively. On the other hand, Eq. (5) recommended by Paulay et al.[1)] agrees pretty well with specimen WF by the ratio of 0.94, but overestimated specimen SF by the ratio of 1.36. Based on these results, make assumption of the strut width W_{ef} to be $0.25dm$ (d_m: diagonal length) gives relatively good estimation for the initial stiffness.

Table 4. Comparison of analytical and experimental initial stiffness

	Exp. stiffness	Calculated stiffness					
		Bare frame		Initial stiffness using diagonal strut model			
Specimen	Initial stiffness (kN/mm)	Initial stiffness (kN/mm)	Ratio	FEMA 306[2] (kN/mm)	Ratio	Paulay et al [1] (kN/mm) $W_{ef} = 0.25d_m$	Ratio
WF	128	18	7.07	68	1.90	136	0.94
SF	150	79	1.91	139	1.08	205	0.73
WM	127	18	7.07	54	2.35	101	1.25
Average			**4.49**		**1.49**		**0.97**

Note : *Ratio = Experimental / Analytical

3.3 Deformation capacity:

In this study, a backbone curve for RC frames with masonry infills is suggested as shown in Figure 8. R_{-crack}, R_{-max} *and* R_u are the representative drift angles at the cracking, the maximum strength and the strength degradation point, respectively, where the strength degradation point is set to be 80% of the maximum strength.

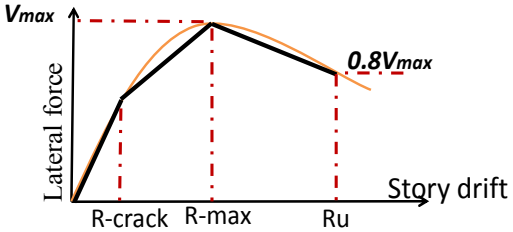

Fig. 8. Idealization of backbone curve

The simplified backbone curves for specimens WF , SF and WM are shown in Figure 9. R-crack is estimated to be 0.1% for all specimens. This indicates that changing frame strength and mortar strength has no significant effect on initial stiffness. The R_{-max} (drift at peak strength), of specimens SF and WF estimated to be 0.8%, but it was found to be 1.5% for specimen WM with weak mortar, which indicates that weak mortar have greater deformation capacity and enhances ductility. For R_u, it was found to be 0.9% and 1.6% for specimen WF and SF, respectively. Therefore, it can be concluded that the influence of surrounding frame strength on R_{-crack} and R_{-max} was slight, but greatly alters the strength degradation slope and R_u. The smooth decrease of strength and

improvement of ductility for specimen SF are considered to be due to the confinement by the stronger surrounding frame, which reduces the inelastic deformation of masonry infill. Specimen WM (Weak mortar) also had almost no degradation of strength even at story drift of 2%.

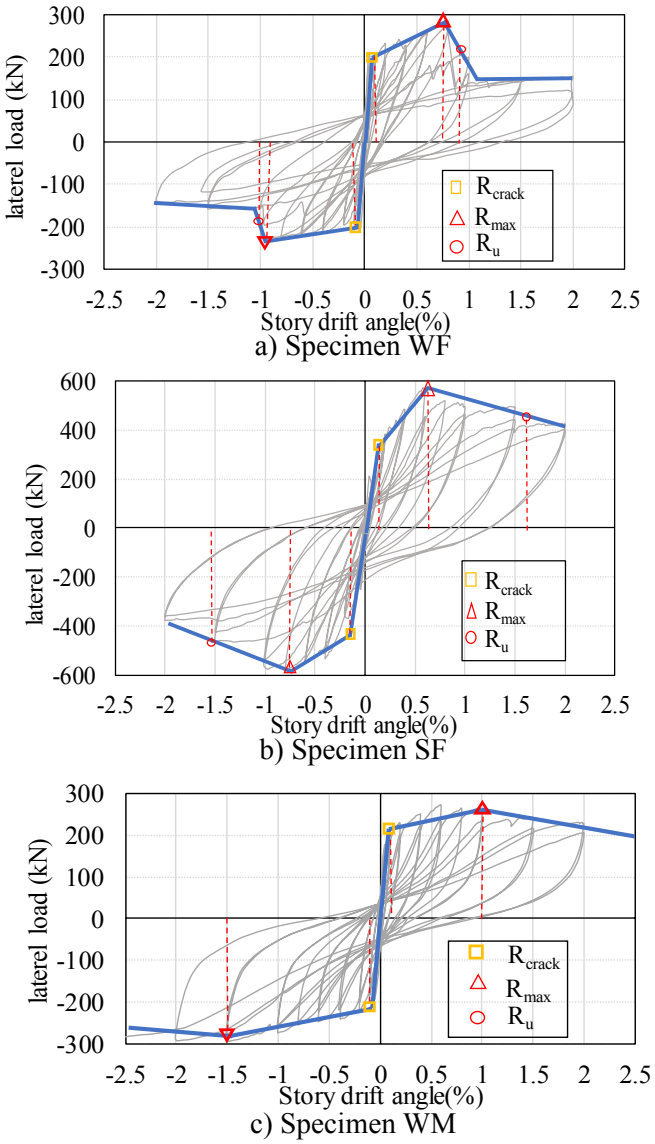

Fig. 9. Backbone curve & deformation limits for specimen: a) WF, b) SF, c) WM

4. CONCLUSION

This paper presents the results of an experimental study and the following are major findings obtained:

a) The experimental results showed that the shear strength of the masonry infill increased by up to 1.5 times when surrounded by a strong frame in comparison to a weaker frame (excluding frame shear strength). This result indicates that the strength of the masonry infill should not be calculated based solely on the results of masonry material testing due to the significant influence of the surrounding frame strength and stiffness.

b) Varying frame strength did not significantly influence the initial stiffness and story drift at max strength. In addition, using simple assumption that masonry infill strut width is 0.25 times its diagonal length gives good estimation of initial stiffness.

c) The post peak degradation slope is much improved in the experimental results with increasing the ratio of frame shear strength to masonry infill. This parameter should be taken into account in the design code of new RC buildings with masonry infill as it can change the brittle behaviour into a more ductile one.

d) Specimen WM with weak mortar showed better deformation capacity with no significant degradation of strength even at story drift of 2%. This indicates that even though low mortar strength reduces the shear strength, it can increase deformation capacity and avoid brittle behaviour of masonry infill.

ACKNOWLEDGMENTS

The study presented in this article was sponsored by the Science and Technology Research Partnership for Sustainable Development (SATREPS) project funded by JST (Japan Science and Technology Agency) and JICA (Japan International Cooperation Agency)for Bangladesh, 2015 project headed by Professor Nakano Yoshiaki, University of Tokyo and it's gratefully acknowledged. Opinions expressed in this article are those of the authors, and do not necessarily represent those of the SATREPS project.

REFERENCES

1) Paulay T, Priestley MJN (1996). *Seismic Design of Reinforced Concrete and Masonry Buildings.* John Wiley & Sons; 1992.
2) FEMA 306 (1998) Evaluation of earthquake damaged concrete and masonry wall buildings, Applied Technology Council (ATC-43 Project)
3) Mehrabi AB, Shing PB, Schuller M, Noland J.(1996)Experimental Evaluation of Masonry-infilled RC Frames. Journal of Structural Engineering, ASCE, Vol. 122, No. 3, March 1996.
4) Wood RH. (1978) Plasticity, Composite Action and Collapse Design of Unreinforced Shear Wall Panels in Frames. Proceeding Institution of Civil Engineering, Part 2, Vol.65,1978, pp.381–411.
5) Mainstone RJ (1971) Summary of Paper 7360: on the stiffness and strength of infilled frames. Proc Inst Civil Eng49:230. doi: 10. 1680/iicep.1971.6267
6) Liauw TC, Kwan KH (1985), Unified Plastic Analysis for Infilled frames. Journal of Structural Engineering, Vol 111, No.7. 1985, pp 1427-1448.
7) Saneinejad A, Hobbs B (1995). Inelastic Design of Infilled Frames. Journal of Structural Engineering, (121)4: 634-650, 1995.
8) Flanagan RD, Bennett RM.(1999) In-Plane Behavior of Structural Clay Tile Infilled Frames. Journal Structural Engineering, Vol. 125, No.6,1999, pp 590–599.
9) American Society of Civil Engineers (ASCE), Seismic Rehabilitation of Existing Buildings. Reston,Virginia, ASCE/SEI 41-06) 2007.
10) Al-Washali H, Suzuki Y, Maeda M. (2016) Seismic Evaluation of Reinforced Concrete Buildings with Masonry Infill Wall. The 16th World Conference of Earthquake Engineering, Chile, 2017.
11) Japanese Industrial Standards (2010).Japanese Standards Association, No. JIS R1250, JIS Z 2201, JIS A 1108, JIS A 1113 (in Japanese)
12) American Society of Testing and Materials (ASTM) (2011). Standard Test Method for Compressive Strength of Masonry Prisms. ASTM C1314, West Conshohocken, PA., 2011.